Chemical Science

rsc.li/chemical-science

ROYAL SOCIETY
OF **CHEMISTRY**

EDGE ARTICLE
Stephan Schulz *et al.*
Modulating the frontier orbitals of L(X)Ga-substituted
diphosphenes [L(X)GaP]$_2$ (X = Cl, Br) and their facile
oxidation to radical cations

Chemical Science

EDGE ARTICLE

Check for updates

All publication charges for this article have been paid for by the Royal Society of Chemistry

Modulating the frontier orbitals of L(X)Ga-substituted diphosphenes [L(X)GaP]2 (X = Cl, Br) and their facile oxidation to radical cations†

Mahendra K. Sharma, [a] Sonia Chabbra, [b] Christoph Wölper,[a] Hanns M. Weinert, [a] Edward J. Reijerse, [b] Alexander Schnegg [b] and Stephan Schulz [*ac]

Modulating the electronic structures of main group element compounds is crucial to control their chemical reactivity. Herein we report on the synthesis, frontier orbital modulation, and one-electron oxidation of two L(X)Ga-substituted diphosphenes [L(X)GaP]2 (X = Cl **2a**, Br **2b**; L = HC[C(Me)N(Ar)]2, Ar = 2,6-i-Pr2C6H3). Photolysis of L(Cl)GaPCO **1** gave [L(Cl)GaP]2 **2a**, which reacted with Me3SiBr with halide exchange to [L(Br)GaP]2 **2b**. Reactions with [Me]NHC ([Me]NHC = 1,3,4,5-tetramethylimidazol-2-ylidene) gave the corresponding carbene-coordinated complexes L(X)GaPP([Me]NHC)Ga(X)L (X = Cl **3a**, Br **3b**). DFT calculations revealed that the carbene coordination modulates the frontier orbitals (*i.e.* HOMO/LUMO) of diphosphenes **2a** and **2b**, thereby affecting the reactivity of **3a** and **3b**. In marked contrast to diphosphenes **2a** and **2b**, the cyclic voltammograms (CVs) of the carbene-coordinated complexes each show one reversible redox event at $E_{1/2}$ = −0.65 V (**3a**) and −0.36 V (**3b**), indicating their one-electron oxidation to the corresponding radical cations as was confirmed by reactions of **3a** and **3b** with the [FeCp2][B(C6F5)4], yielding the radical cations [L(X)GaPP([Me]NHC)Ga(X)L]B(C6F5)4 (X = Cl **4a**, Br **4b**). The unpaired spin in **4a** (79%) and **4b** (80%) is mainly located at the carbene-uncoordinated phosphorus atoms as was revealed by DFT calculations and furthermore experimentally proven in reactions with [n]Bu3SnH, yielding the diphosphane cations [L(X)GaPHP([Me]NHC)Ga(X)L]B(C6F5)4 (X = Cl **5a**, Br **5b**). Compounds **2–5** were fully characterized by NMR and IR spectroscopy as well as by single crystal X-ray diffraction (sc-XRD), and compounds **4a** and **4b** were further studied by EPR spectroscopy, while their bonding nature was investigated by DFT calculations.

Introduction

Stable radicals of main-group elements have attracted significant interest due to their interesting electronic nature, bonding situation, reactivity, and physical properties, which render them promising reagents in synthetic chemistry and materials science.[1] Therefore, the isolation of stable main-group element radicals is of high interest and many stable main-group element-based radicals have been reported in recent years,[1,2] including kinetically-stabilized neutral,[3] anionic,[4] and cationic[5] phosphorous-centered radicals. The use of sterically

demanding ligands and/or singlet carbenes such as N-heterocyclic carbenes (NHCs) and cyclic (alkyl)(amino)-carbenes (cAACs) as well as π-delocalization of the unpaired electron spin density have been proven to stabilize these radicals. Phosphorus-centred radical cations Trip2(R)P[•+] **I** (R = iPr3C6H2, Me3C6H2) and tetraaryldiphosphane radical cation (Trip2-PPTrip2)[•+] **II** (Trip = iPr3C6H2) were isolated by one-electron oxidation of the corresponding (di)phosphanes (Fig. 1),[5a,b] whereas base-stabilized radical cations **III–VI** were isolated using strong σ-donor NHCs, cAACs and N-heterocyclic vinylidenes (NHV, **IX**), respectively.[5c,e,5l,10a] In addition, four-membered π-delocalized cyclic radical cations **VII** and **VIII** as well as several metal-coordinated radical compounds (**X**, **XI**) were reported.[5k,m,n,11a,12]

Diphosphenes (RPPR) containing a P–P double bond are analogues to alkenes and have received substantial fundamental interest in molecular main-group chemistry due to their small HOMO–LUMO energy gaps compared to alkenes, resulting in an increased reactivity and potential applicability in synthetic chemistry.[6] In 1981, Yoshifuji *et al.* isolated the first stable diphosphene, [Mes*P═PMes*] (Mes* = 2,4,6-t-Bu3-

[a]*Institute of Inorganic Chemistry, University of Duisburg-Essen, Universitätsstraße 5-7, D-45141, Essen, Germany. E-mail: stephan.schulz@uni-due.de; Web: https://www.uni-due.de/ak_schulz/index_en.php*

[b]*EPR Research Group, Max Planck Institute for Chemical Energy Conversion, Stiftstrasse 34-36, Mülheim an der Ruhr, D-45470, Germany*

[c]*Center for Nanointegration Duisburg-Essen (CENIDE), University of Duisburg-Essen, Carl-Benz-Straße 199, 47057 Duisburg, Germany*
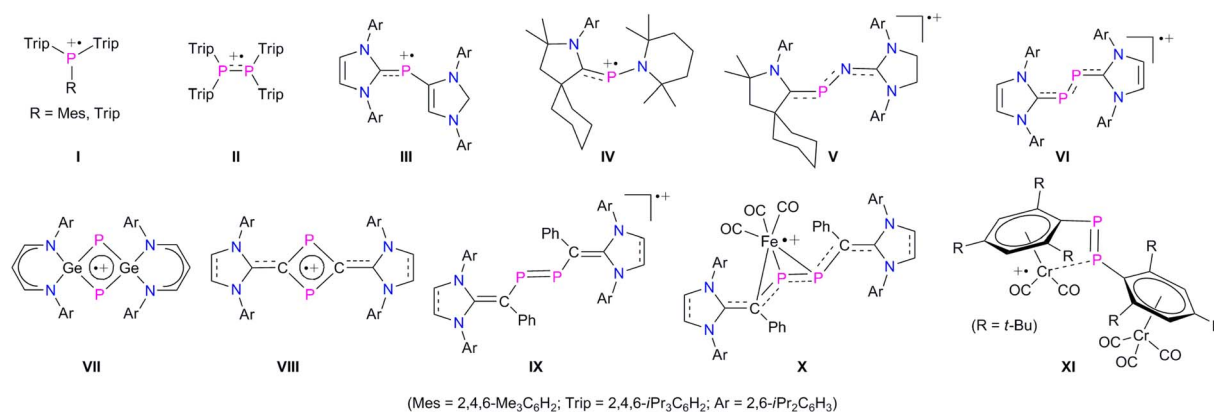
Fig. 1 Selected examples of phosphorus radical cations **I–VIII**, diphosphene radical cation **IX**, diphosphene stabilized metal-centered radical cations **X–XI**, and L(X)Ga-substituted diphosphenes radical cations (this work).

C_6H_2),[7] followed by subsequent reports on other kinetically stabilized diphosphenes.[8] In general, the LUMO of diphosphenes typically consists of the low-lying π^* orbital of the P=P double bond, whereas the HOMO comprises the electron lone pair orbital of the phosphorus atoms.[6–8] Therefore, one-electron reduction of diphosphenes to the corresponding radical anions is feasible.[9] In marked contrast, the one-electron oxidation to the corresponding radical cations remains a challenging task.[6–8] To the best of our knowledge, the divinyldiphosphene radical cations $[\{(NHC)C(Ph)\}P]_2^{\bullet+}$ (**IX**) reported by Ghadwal et al. represent the only genuine example (Fig. 1),[10] whereas radical cations **X** and **XI** are rather metal-centered radical cations according to quantum chemical calculations (Fig. 1).[11,12]

The scarcity of diphosphene radical cations as well as our general interest in the reactivity of L(X)Ga-substituted, electron-rich dipnictenes[13] prompted us to synthesize L(X)Ga-substituted diphosphenes and investigate their redox properties. We herein report on the synthesis of two L(X)Ga-substituted diphosphenes $[L(X)GaP]_2$ (X = Cl **2a**, Br **2b**) and their reactions with an N-heterocyclic carbene. Carbene-coordination in **3a** and **3b** resulted in a modulation of their frontier orbitals with respect to those of the uncoordinated diphosphenes, allowing one-electron oxidation reactions to the corresponding diphosphene radical cations $[L(X)GaPP(^{Me}NHC)$ $Ga(X)L]B(C_6F_5)_4$ (X = Cl **4a**, Br **4b**, Fig. 1). Radical cations **4a** and **4b** further react with $^nBu_3SnH$ to diphosphane cations **5a** and **5b**, respectively.

Results and discussion

Phosphaketenes (RPCO) contain weak P–CO bonds and readily undergo decarbonylation upon photolysis, thermolysis and in reactions with Lewis bases.[14] We recently prepared the

gallaphosphaketene L(Cl)GaPCO **1** and reported on its decarbonylation reaction with LGa to an unprecedented gallaphosphene L(Cl)GaPGaL and its remarkable activity in small molecule activation.[15] We here extended our studies to the photolysis of **1**. UV treatment of a colorless toluene solution of **1** occurred with decarbonylation at ambient temperature and yielded the desired L(Cl)Ga-substituted diphosphene [L(Cl)GaP]$_2$ **2a** in 65% isolated yield, which reacted with an excess of Me$_3$SiBr with halide exchange and quantitative formation of $[L(Br)GaP]_2$ **2b** (Scheme 1).

Diphosphenes **2a** and **2b** are green crystalline solids, which are stable in solution and solid states under inert gas atmosphere and poorly soluble in common organic solvents such as THF, toluene, fluorobenzene, benzene, and n-hexane. Their ^1H and $^{13}C\{^1H\}$ NMR spectra each exhibit one set of resonances for the β-diketiminate ligand, indicating a symmetric nature of the molecules in solution. The $^{31}P\{^1H\}$ NMR spectrum of **2a** (+761.6 ppm) and **2b** (+766.8 ppm) each displays a sharp singlet for the phosphorus atoms, which are consistent with the previously reported metal-substituted diphosphenes.[16] The solid-state molecular structures of **2a** and **2b** (Fig. 2) revealed trans-bent geometries along the P–P double bonds. Both compounds reside at a crystallographic center of inversion and crystallize in the monoclinic space group $P2_1/n$.[17] The phosphorus atoms are twofold- and the gallium atoms fourfold-coordinated. The P1–
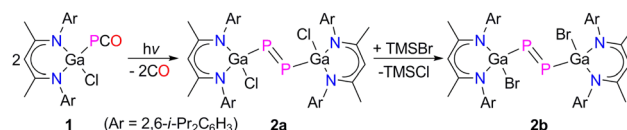
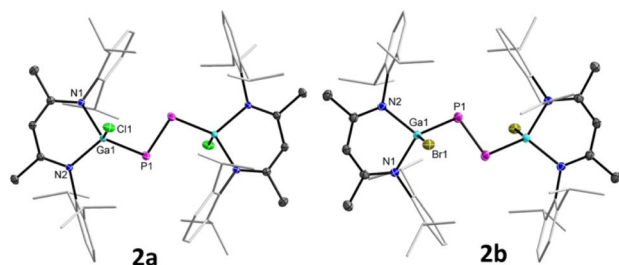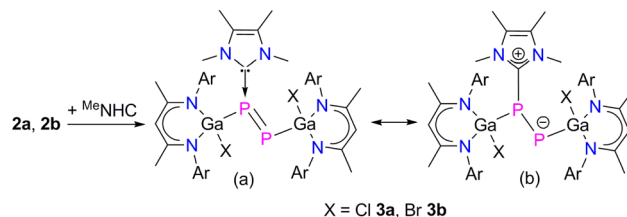**Scheme 1** Synthesis of diphosphenes **2a** and **2b**.

Fig. 2 Molecular structures of **2a** and **2b**. Ellipsoids set at 50% probability; hydrogen atoms and alternate positions of the disordered parts (in **2a**) are omitted for clarity. Symmetry operations used to generate equivalent atoms: $-x$, $-y$, $-z + 1$ (**2a**), and $-x + 1$, $-y$, $-z$ (**2b**).

Scheme 2 Synthesis of ^{Me}NHC-diphosphenes **3** (a), and likely resonance structures (b).

P1$'$ bond lengths of **2a** (2.0381(5) Å) and **2b** (2.0282(8) Å) are in the typical range of diphosphenes (2.02–2.08 Å)[6–8] and agree well with sum of the calculated P–P double-bond radii (2.04 Å).[18a] The Ga–X bond lengths of **2a** (X = Cl, 2.2207(3) Å) and **2b** (X = Br, 2.3680(2) Å) are comparable to those of LGaX$_2$ [X = Cl 2.218(1), 2.228(1) Å; Br 2.286(1), 2.330(1) Å].[19]

To gain further insights into the electronic structures of compounds **2a** and **2b**, we performed DFT calculations at the B3LYP-D3BJ/def2-TZVP level of theory.[20] The DFT optimized geometries of compounds **2** are in good agreement with their solid-state molecular structures (Tables 1 and S4†). The calculations revealed that the HOMO of **2a** (-5.22 eV) and **2b** (-5.26 eV) each corresponds to the Ga–P σ-bonds with a small contribution from the non-bonding electron lone pair of the P atoms, while the HOMO-3 (-6.23 eV **2a**, -6.28 eV **2b**) involves the π type orbital of the P–P double bond (Fig. 4, and S47 and S48†) and the LUMOs (-2.37 eV **2a**, -2.44 eV **2b**) are mainly the π* orbital of the P–P double bond. Due to our general interest in the redox properties of L(X)Ga-substituted dipnictenes,[21] we measured the cyclic voltammograms (CVs) of **2a** and **2b**. Both compounds exhibited two irreversible reduction events at $E_{pc} = -2.30$, -2.78 V (**2a**) and -2.07, -2.58 V (**2b**) vs. Fc/Fc$^+$, respectively, which can be assigned to the corresponding radical anions and dianions (Fig. S29 and S30†). Unfortunately, all attempts to reduce **2a** and **2b** failed and yielded only LGa as the main product.

Since NHCs are known as strong σ-donor ligands, which have been reported to enhance the reactivity of diphosphenes,[22] we reacted compounds **2a** and **2b** with ^{Me}NHC (^{Me}NHC = 1,3,4,5-tetramethylimidazol-2-ylidene). The reaction proceeded

at ambient temperature with an immediate color change from green to red and formation of the corresponding ^{Me}NHC-coordinated diphosphenes L(X)GaPP(^{Me}NHC)Ga(x)L (X = Cl **3a**, Br **3b**) in high (>92%) yields (Scheme 2). Compounds **3a** and **3b** are soluble in common organic solvents and stable under argon atmosphere at ambient temperature, but rapidly decompose upon exposure to air. The ^{1}H and ^{13}C{^{1}H} NMR spectra of compounds **3a** and **3b** exhibit two distinct sets of resonances for the β-diketiminate ligand as was observed for L(X)Ga-substituted dipnictenes,[13] dipnictanes,[23] gallapnictenes,[15a,24] and other complexes.[25] The ^{31}P{^{1}H} NMR spectra of **3a** (-85.8 ppm, $^1J_{PP} = 353.0$ Hz, and -258.5 ppm, $^1J_{PP} = 353.0$ Hz) and **3b** (-77.7 ppm, $^1J_{PP} = 358.9$ Hz, and -247.5 ppm, $^1J_{PP} = 358.9$ Hz) each display two doublets for the electronically nonequivalent phosphorus atoms, which are upfield shifted with respect to diphosphenes **2a** (+761.6 ppm) and **2b** (+766.8 ppm).

The molecular structures of complexes **3a** and **3b** in the solid state confirmed the carbene coordination to only one phosphorus atom and revealed a similar trans-bent geometry along the P–P double bond as was observed for **2a** and **2b** (Fig. 3).

Compound **3a** crystallizes in the triclinic space group $P\bar{1}$ and **3b** in the monoclinic space group $P2_1/n$.[17] The P1–P2 bond lengths in **3a** (2.1871(8)/2.1835(8) Å) and **3b** (2.1623(5) Å) are significantly elongated compared to those of diphosphenes **2a** (2.0381(5) Å) and **2b** (2.0282(8) Å), but still shorter than the calculated P–P single bond length (2.22 Å).[18b] The Ga1–P1 bonds in **3a** (2.3328(7)/2.3433(6) Å) and **3b** (2.3205(4) Å) are slightly elongated and the Ga2–P2 bonds slightly shortened (**3a** 2.2747(6)/2.2695(7) Å, **3b** 2.2664(4) Å) compared to those in diphosphenes **2a** and **2b** (Table 1), respectively; but they are comparable to the sum of the calculated Ga–P single-bond radii[18b] and previously reported Ga–P single bond lengths.[15]

Table 1 Selected bond lengths (Å) of compounds **2–5**. DFT optimized values are shown in square brackets

|	P1–P2/P1$'$	Ga1–P1	Ga2–P2/P1$'$	P1–C59
2a	2.0381(5) [2.040]	2.3131(3) [2.332]	2.3131(3) [2.334]	—
3a	2.1871(8)/2.1835(8) [2.158]	2.3328(7)/2.3433(6) [2.325]	2.2747(6)/2.2695(7) [2.280]	1.862(2)/1.864(2) [1.852]
4a	2.142(8) [2.130]	2.3479(13) [2.358]	2.3456(10) [2.354]	1.823(3) [1.816]
5a	2.2227(14)	2.3655(16)	2.3466(16)	1.838(4)
2b	2.0282(8) [2.040]	2.3120(4) [2.333]	2.3120(4) [2.333]	—
3b	2.1623(5) [2.158]	2.3205(4) [2.327]	2.2664(4) [2.280]	1.8570(13) [1.852]
4b	2.1336(7) [2.133]	2.3591(8) [2.359]	2.3522(7) [2.357]	1.8262(19) [1.817]
5b	2.223(3)	2.367(3)	2.339(3)	1.829(8)
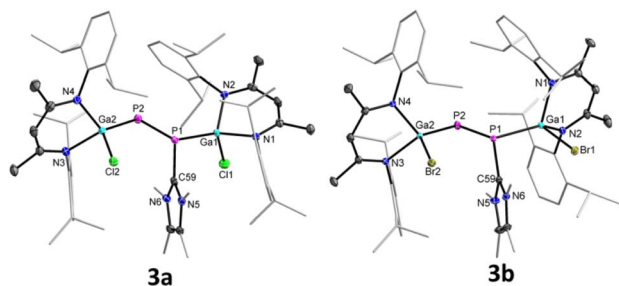
Fig. 3 Molecular structures of **3a** and **3b**. Ellipsoids set at 50% probability; hydrogen atoms, alternate positions of the disordered parts (in **3b**) are omitted for clarity.
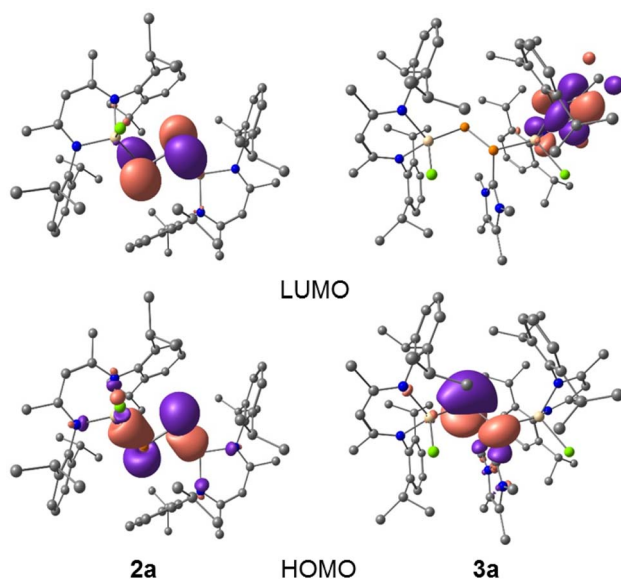

Fig. 4 HOMO and LUMO of compounds **2a** and **3a** calculated at B3LYP-D3BJ/def2-TZVP level of theory (isovalue 0.0432 a.u.). Hydrogen atoms are omitted for clarity.

DFT calculations at the B3LYP-D3BJ/def2-TZVP level of theory[20] revealed that the HOMOs of complexes **3a** and **3b** are mainly composed of *p*-type orbitals of the two-fold-coordinated phosphorus atoms (P2), while the LUMOs are predominantly located on the ligand backbone (Fig. 4, S49 and S50†).

The electron donation from ^{Me}NHC to the π^*-orbitals of **2a** and **2b** leads to charge separation between the P atoms, hence, the P2 atoms show higher negative NPA charges (**3a** −0.84e, **3b** −0.83e) than the P1 atoms (**3a** −0.09e, **3b** −0.09e). The P–P bond in **3a** and **3b** reflects single bond character with less π-bonding contribution than in the diphosphenes **2a** and **2b**, as was confirmed by quantum chemical calculations. Calculated MBOs (Mayer bond orders) for the P1–P2 bond of **2a** (1.881) and **2b** (1.883) are significantly larger than for **3a** (1.208) and **3b** (1.219), respectively, hence the electronic situation in **3a** and **3b** is best illustrated by the zwitterionic structure depicted in Scheme 2. In addition, the ^{Me}NHC coordination significantly reduces the HOMO–LUMO energy gap of diphosphenes **2a** (−7.60 eV) and **2b** (−7.70 eV) to −5.25 eV (**3a**) and −5.32 eV (**3b**),

respectively. The HOMOs of **3a** (−3.91 eV) and **3b** (−3.95 eV) are high-lying and therefore expected to allow the oxidation of **3a** and **3b** to the corresponding radical cations.

We therefore measured CVs of **3a** and **3b** to get deeper insights into their redox properties. The CVs of **3a** (Fig. S31†) and **3b** (Fig. S32†) each show one reversible redox event at $E_{1/2} =$ −0.65 V and −0.36 V *vs.* Fc/Fc$^+$, respectively, which are fully consistent with their one-electron oxidation to the corresponding radical cations. It is worth mentioning here that the ^{Me}NHC coordination not only changed the frontier orbitals of **2a** and **2b** in compounds **3a** and **3b**, respectively, but also significantly altered their redox properties (see above). Indeed, reactions of **3a** and **3b** with [FeCp$_2$][B(C$_6$F$_5$)$_4$] gave the radical cations [L(X)GaPP(^{Me}NHC)Ga(X)L][B(C$_6$F$_5$)$_4$] (X = Cl **4a**, Br **4b**) as yellow crystalline solids in good yields (Scheme 3). Compounds **4a** and **4b** are soluble in common organic solvents (toluene, fluorobenzene, THF) and stable under an inert gas atmosphere at ambient temperature, but rapidly decompose when exposed to air and moisture.

The molecular structures of **4a** and **4b** were determined by sc-XRD (Fig. 5). Suitable single crystals were obtained upon storage of saturated toluene solutions of **4a** and **4b** at ambient temperature. Compound **4a** crystallizes in the triclinic space group $P\bar{1}$ and **4b** in the monoclinic space group $P2_1/c$.[17]

Upon one-electron oxidation, the P1–P2 bond lengths of the NHC-coordinated complexes **3a** (2.1871(8) Å) and **3b** (2.1623(5) Å) became slightly shorter in the radical cations **4a** (2.1423(8) Å) and **4b** (2.1336(7) Å), which is most likely caused by the slight delocalization of the unpaired electron within the P$_2$ unit (see below). Despite the slightly increased π-bonding contribution in the radical cations **4a** and **4b** compared to the carbene-coordinated complexes **3a** and **3b**, the unpaired electrons in **4a** and **4b** are mostly located at the carbene-free P atoms. **4a** and **4b** are therefore best described as phosphorus-centered radicals, in which the delocalization of the unpaired electron is disturbed by the coordination of NHC. The Ga1–P1 bonds in **4a** (2.3479(13) Å) and **4b** (2.3591(8) Å) are virtually identical with those of **3a** (2.3328(7) Å) and **3b** (2.3205(4) Å), whereas the Ga2–P2 bonds in **4a** (2.3456(10) Å) and **4b** (2.3522(7) Å) are substantially elongated compared to those of **3a** (2.2747(6) Å) and **3b** (2.2664(4) Å), respectively. In compounds **3a** and **3b**, the P2 atoms are far more negatively charged (−0.84 **3a**, −0.84 **3b**) than those in **4a** (−0.33) and **4b** (−0.32), respectively, which rather contain only one unpaired electron (Table S6†). Therefore, the short Ga2–P2 bond lengths in **3a** and **3b** most likely result from electrostatic attractions between the negatively charged P and positively charged Ga atoms. The P1–C59 bonds
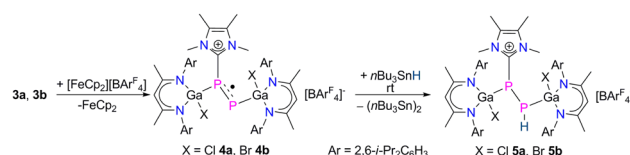
Scheme 3 One-electron oxidation of compounds **3** to radical cations **4** and reactions of **4** with *n*Bu$_3$SnH.
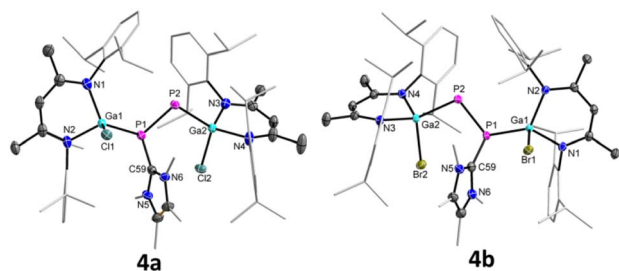
Fig. 5 Molecular structures of radical cations **4a** and **4b**. Ellipsoids set at 50% probability; hydrogen atoms, alternate positions of the disordered parts, anion (BAr$^F_4$), and solvent molecule (toluene in **4b**) are omitted for clarity.

Fig. 6 X-band CW EPR spectra of **4a** (black), **4b** (blue) and corresponding simulations in red at (A) 290 K and (B) 80 K. Simulation parameters for 290 K: $g_{iso} = 2.015$, $^{Ga}A_{iso} = 92.6$ MHz and -59.7 MHz, $^PA_{iso} = 298.7$ MHz and 192.7 MHz. For **4a** and **4b** the same parameters were used except the Lorentzian full width at half maximum (FWHM) linewidth, which was adjusted to 2.25 mT (**4a**) and 2.5 mT (**4b**). Simulation parameters for 80 K: $g_{iso} = 2.017$, $^{Ga}A = [72.2, 104.4, 72.7]$ MHz and $[-98.1, -21.2, -95.3]$ MHz, $^PA = [255.9, 229.9, 352.0]$ MHz and $[-114.4, -55.3, 595.0]$ MHz and Lorentzian FWHM linewidths of 2.06 mT (**4a**) and 2.8 mT (**4b**).

in **4a** (1.823(3) Å) and **4b** (1.8262(19) Å) are rather contracted compared to those of **3a** (1.862(2) Å) and **3b** (1.8570(13) Å), in accordance with an increased electron density transfer from the carbene carbon atom to the coordinated P atom in **4a** and **4b** upon oxidation.

The DFT optimized geometries of compounds **2–4** are in good agreement with their solid-state molecular structures (Tables 1 and S4†).[17,20] The calculated MBOs (Mayer bond orders) for the P1–P2 bond of **2a** (1.8810), **2b** (1.8830), **3a** (1.2075), **3b** (1.2193), **4a** (1.2938), and **4b** (1.2534) are fully consistent with the experimentally observed changes of the P–P bond lengths (Tables 1 and S4†).[26] Similarly, the MBOs for the P1–C59 bond of **3a** (1.0712), **3b** (1.0670), **4a** (1.0013), and **4b** (1.0268) exhibit the expected trend (Tables 1 and S4†). Upon one-electron oxidation, the HOMOs of **3a** and **3b** become the corresponding SOMOs in the radicals **4a** and **4b**, while the LUMO remains the same. Furthermore, the topology of the SOMOs in **4a** and **4b** also remains identical to the HOMO of **3a** and **3b**.

To gain additional insight into the electronic structures of radicals **4a** and **4b**, Spin Hamiltonian (SH) parameters (g- and hyperfine (A)-tensors with main values $[g_x, g_y, g_z]$ and $[A_x, A_y, A_z]$, respectively) were obtained from quantum chemical calculations and compared to experimental values obtained from EPR spectroscopy. Fig. 6 depicts continuous wave (CW) X-band EPR spectra of **4a** and **4b** measured in a 1 : 9 solution of fluorobenzene and toluene at 290 K (A) and 80 K (B), respectively. The 290 K multi-line spectra centered at an effective $g = 2.015 \pm 0.002$ is assigned to hyperfine splitting of the unpaired electron with two ^{31}P nuclei ($I = 1/2$) and two $^{69/71}Ga$ nuclei ($I = 3/2$). At room temperature, the splittings in the EPR spectra are dominated by the isotropic part of the A-tensors since their anisotropies are averaged by rotational motion of the molecules. In the frozen solution spectra obtained at 80 K, all components of the g- and A-tensors contribute to the EPR spectrum. Due to the large number of couplings, an overall less structured spectrum and an increase of the total linewidth by 60%, as compared to the 290 K spectrum, is observed.

EPR spectra at 290 K and 80 K were successfully simulated using isotropic g-values (g_{iso}) and isotropic (A_{iso} for 290 K) and anisotropic A-tensors (for 80 K) for the phosphorus and gallium atoms, respectively (Fig. 6, and Table S10†). Here, the A-tensor
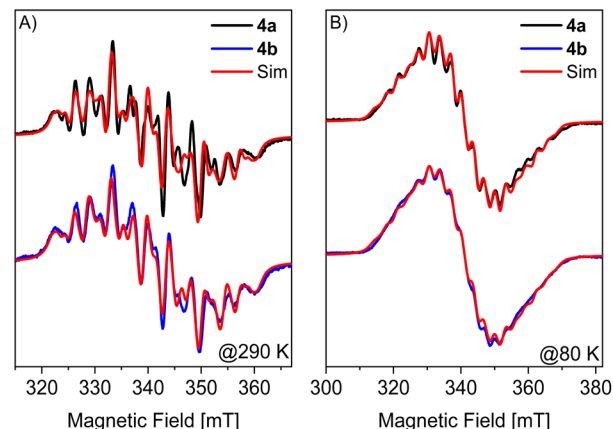
of the ^{69}Ga (i.e., highest natural abundance of 60.11%) isotope is reported. The corresponding values of the ^{71}Ga isotope (39.89% natural abundance) can be obtained by scaling the nuclear gyromagnetic ratios of the two isotopes $A(^{71}Ga) = A(^{69}Ga)g_n(^{71}Ga)/g_n(^{69}Ga) = A(^{69}Ga) \times 1.2706$. Despite an overall satisfying match between experiment and simulation the obtained A_{iso} for the different nuclei (and isotopes) was found to differ for liquid and frozen solution spectra, which likely originates from a strong correlation of the different A-tensor components in the fit.

The calculated Mulliken atomic spin-populations and the plots of SOMO (at B3LYP-D3BJ/def2-TZVP level of theory)[20] suggest that the unpaired electron in **4a** (79.7%) and **4b** (80.4%) are mainly localized in the p-orbitals of the twofold-coordinated phosphorus atoms (P2) with smaller contributions at P1 (**4a** 12.2% and **4b** 11.7%). The individual SOMO p-populations are
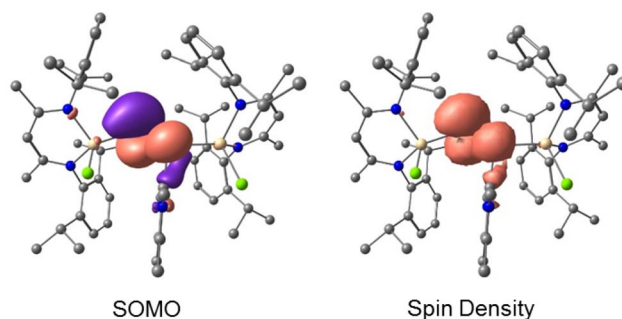

Fig. 7 Calculated SOMO (isovalue 0.0432 a.u.) and spin-density distribution (isovalue 0.0025 a.u.) of radical cation **4a** at the B3LYP-D3BJ/ZORA-def2-TZVPP level of theory. Hydrogen atoms are omitted for clarity.

given in Table S11.† The spin-population at the gallium and the carbene carbon atoms is very small. However, the total electron spin-densities are covering both phosphorus atoms (Fig. 7).

To further assign the A-tensors derived from EPR spectra of **4a** and **4b** to their two P and Ga atoms, experimental values were compared to theoretical values obtained by DFT calculations (Table S10†). This comparison allows for a tentative assignment of the most anisotropic ^{31}P A-tensor to P2 (consistent with the large p-orbital contribution to the spin population), while P1 is assumed to exhibit a large and less anisotropic A-tensor. The assignment of the Ga1 HFI to the most isotropic tensor seems to be straightforward since the correspondence between the DFT predicted values and the experimental ones is good (Table S10†). However, the situation for Ga2 is somewhat ambiguous. The DFT calculations predict a tensor with axial anisotropy and smaller values as compared to Ga1. The experimental values are, however, relatively large but do show an axial anisotropy. Possibly, the isotropic component in the fits of the frozen solution spectra is overestimated.

To probe the chemical reactivity of radical cations **4a** and **4b**, we reacted them with a slight excess of nBu$_3$SnH in fluorobenzene at ambient temperature. The solutions of **4a** and **4b** immediately turned colorless and diphosphanes **5a** and **5b** were isolated as colorless crystalline solids. The ^{1}H (Fig. S19 and S24†) and ^{31}P (Fig. S21, S22, S26 and S27†) NMR spectra of both **5a** and **5b** display the expected signals of the β-diketiminate ligand and the carbene unit. The ^{31}P NMR spectra of **5a** (−147.5 ppm) (dd, $^1J_{PP}$ = 85.3, $^2J_{PH}$ = 25.3 Hz) and −228.0 ppm (dd, $^1J_{PP}$ = 85.3, $^1J_{PH}$ = 180.9 Hz), and **5b** (−142.4 ppm) (dd, $^1J_{PP}$ = 88.2, $^2J_{PH}$ = 24.7 Hz) and −225.3 ppm (dd, $^1J_{PP}$ = 88.2, $^1J_{PH}$ = 181.1 Hz) both exhibited doublets of doublets for the P–H units, while the same resonances in the ^{1}H NMR spectra overlapped with the signals of the β-diketiminate ligand and therefore could not be assigned. The molecular structures of compounds **5a** and **5b** were confirmed by sc-XRD (Fig. S45 and S46†). Both compounds crystallized in the triclinic space group $P\bar{1}$.[17] The P1–P2 bond lengths in **5a** (2.223(1) Å), and **5b** (2.223(3) Å) are significantly elongated compared to the radical cations **4a** (2.142(8) Å) and **4b** (2.134(7) Å), respectively, and are consistent with the calculated P–P single bond radii (2.22 Å)[18b] and previously reported P–P single bond lengths.[27] More important, the isolation of compounds **5a** and **5b** clearly confirmed that the unpaired spin in radical cations **4a** and **4b** is mainly localized at the carbene-free phosphorus atom (P2).

Conclusions

L(X)Ga-substituted diphosphenes **2a** and **2b** reacted with ^{Me}NHC to the corresponding ^{Me}NHC-coordinated complexes **3a** and **3b**. In contrast to compounds **2a** and **2b**, the ^{Me}NHC-coordinated complexes **3a** and **3b** reacted in one-electron oxidation reactions to the corresponding radical cations **4a** and **4b**. Quantum chemical calculations and EPR spectroscopy revealed that the spin-population in **4a** and **4b** mainly resides at carbene-free phosphorus atoms (P2), which was further confirmed in reactions with nBu$_3$SnH, yielding diphosphanes **5a** and **5b**, respectively. The study emphasizes on the reactivity enhancement of diphosphenes using a carbene to isolate the cationic P-centered radicals. As a variety of carbenes with different donor properties are available, the reactivity of dipnictenes can likely be tuned and various dipnictene radicals may be isolated in the future.

Data availability

Crystallographic data for all compounds (**2a/b–4a/b**) has been deposited at the CCDC under 2184009–2184012, 2184019, 2184020, 2184142 and 2184320. Additional analytical datasets supporting this article have been uploaded as part of the ESI.†

Author contributions

MKS performed the experiments and wrote the manuscript draft, HMW performed CV experiments and CW the sc-XRD studies, SS supervised the work and finalized the manuscript. EPR data was measured by SC and analyzed by SC, ER and AS. DFT calculations were performed and analysed by ER. SC, ER and AS jointly wrote the EPR and DFT sections.

Conflicts of interest

There are no conflicts to declare.

References

1 (a) R. G. Hicks, *Stable Radicals: Fundamentals and Applied Aspects of Odd-Electron Compounds*, John Wiley & Sons Ltd, Chichester, 2010; (b) P. P. Power, *Chem. Rev.*, 2003, **103**, 789–809; (c) J. Konu and T. Chivers, *Stable Radicals: Fundamental and Applied Aspects of Odd-Electron Compounds*, R. G. Hicks, John Wiley & Sons, Ltd, 2010, pp. 381–406; (d) P. P. Power, *Nature*, 2010, **463**, 171–177; (e) G. W. Tan and X. P. Wang, *Chin. J. Chem.*, 2018, **36**, 573–586; (f) V. Y. Lee, M. Nakamoto and A. Sekiguchi, *Chem. Lett.*, 2008, **37**, 128–133.

2 (a) S. Kundu, S. Sinhababu, V. Chandrasekhar and H. W. Roesky, *Chem. Sci.*, 2019, **10**, 4727–4741; (b) K. C. Mondal, S. Roy and H. W. Roesky, *Chem. Soc. Rev.*, 2016, **45**, 1080–1111; (c) Y. Su and R. Kinjo, *Coord. Chem. Rev.*, 2017, **352**, 346–378; (d) Y. Kim and E. Lee, *Chem.–Eur. J.*, 2018, **24**, 19110–19121; (e) M. Soleilhavoup and G. Bertrand, *Acc. Chem. Res.*, 2015, **48**, 256–266; (f) C. D. Martin, M. Soleilhavoup and G. Bertrand, *Chem. Sci.*, 2013, **4**, 3020–3030; (g) F. Breher, *Coord. Chem. Rev.*, 2007, **251**, 1007–1043; (h) H. Grützmacher and F. Breher, *Angew. Chem., Int. Ed.*, 2002, **41**, 4006–4011; (i) C. Helling and S. Schulz, *Eur. J. Inorg. Chem.*, 2020, **34**, 3209–3221.

3 For neutral phosphorus radicals: (a) S. L. Hinchley, C. A. Morrison, D. W. H. Rankin, C. L. B. Macdonald, R. J. Wiacek, A. H. Cowley, M. F. Lappert, G. Gundersen, J. A. C. Clyburne and P. P. Power, *Chem. Commun.*, 2000, 2045–2046; (b) A. Armstrong, T. Chivers, M. Parvez and R. T. Boeré, *Angew. Chem., Int. Ed.*, 2004, **43**, 502–505; (c) S. Ito, M. Kikuchi, M. Yoshifuji, A. J. Arduengo III, T. A. Konovalova and L. D. Kispert, *Angew. Chem., Int. Ed.*, 2006, **45**, 4341–4345; (d) P. Agarwal, N. A. Piro, K. Meyer, P. Müller and C. C. Cummins, *Angew. Chem., Int. Ed.*, 2007, **46**, 3111–3114; (e) O. Back, B. Donnadieu, M. von Hopffgarten, S. Klein, R. Tonner, G. Frenking and G. Bertrand, *Chem. Sci.*, 2011, **2**, 858–861; (f) T. Beweries, R. Kuzora, U. Rosenthal, A. Schulz and A. Villinger, *Angew. Chem., Int. Ed.*, 2011, **50**, 8974–8978; (g) A. Hinz, A. Schulz and A. Villinger, *Angew. Chem., Int. Ed.*, 2015, **54**, 668–672; (h) L. Gu, Y. Zheng, E. Haldón, R. Goddard, E. Bill, W. Thiel and M. Alcarazo, *Angew. Chem., Int. Ed.*, 2017, **56**, 8790–8794; (i) X. Chen, A. Hinz, J. R. Harmer and Z. Li, *Dalton Trans.*, 2019, **48**, 2549–2553; (j) Z. Li, Y. Hou, Y. Li, A. Hinz, J. R. Harmer, C.-Y. Su, G. Bertrand and H. Grützmacher, *Angew. Chem., Int. Ed.*, 2018, **57**, 198–202; (k) A. M. Tondreau, Z. Benkő, J. R. Harmer and H. Grützmacher, *Chem. Sci.*, 2014, **5**, 1545–1554; (l) M. Scheer, C. Kuntz, M. Stubenhofer, M. Linseis, R. F. Winter and M. Sierka, *Angew. Chem., Int. Ed.*, 2009, **48**, 2600–2604; (m) S. Ishida, F. Hirakawa and T. Iwamoto, *J. Am. Chem. Soc.*, 2011, **133**, 12968–12971.

4 For phosphorus radical anions: (a) T. Cantat, F. Biaso, A. Momin, L. Ricard, M. Geoffroy, N. Mézailles and P. Le Floch, *Chem. Commun.*, 2008, 874–876; (b) C. Pi, Y. Wang, W. Zheng, L. Wan, H. Wu, L. Weng, L. Wu, Q. Li and P. v. R. Schleyer, *Angew. Chem., Int. Ed.*, 2010, **49**, 1842–1845; (c) X. Pan, X. Wang, Y. Zhao, Y. Sui and X. Wang, *J. Am. Chem. Soc.*, 2014, **136**, 9834–9837; (d) G. Tan, S. Li, S. Chen, Y. Sui, Y. Zhao and X. Wang, *J. Am. Chem. Soc.*, 2016, **138**, 6735–6738.

5 For phosphorus radical cations: (a) X. Pan, X. Chen, T. Li, Y. Li and X. Wang, *J. Am. Chem. Soc.*, 2013, **135**, 3414–3417; (b) X. Pan, Y. Su, X. Chen, Y. Zhao, Y. Li, J. Zuo and X. Wang, *J. Am. Chem. Soc.*, 2013, **135**, 5561–5564; (c) O. Back, M. A. Celik, G. Frenking, M. Melaimi, B. Donnadieu and G. Bertrand, *J. Am. Chem. Soc.*, 2010, **132**, 10262–10263; (d) O. Back, B. Donnadieu, P. Parameswaran, G. Frenking and G. Bertrand, *Nat. Chem.*, 2010, **2**, 369–373; (e) R. Kinjo, B. Donnadieu and G. Bertrand, *Angew. Chem., Int. Ed.*, 2010, **49**, 5930–5933; (f) Y. Su, X. Zheng, X. Wang, X. Zhang, Y. Sui and X. Wang, *J. Am. Chem. Soc.*, 2014, **136**, 6251–6254; (g) A. Brückner, A. Hinz, J. B. Priebe, A. Schulz and A. Villinger, *Angew. Chem., Int. Ed.*, 2015, **54**, 7426–7430; (h) X. Pan, X. Wang, Z. Zhang and X. Wang, *Dalton Trans.*, 2015, **44**, 15099–15102; (i) G. Ménard, J. A. Hatnean, H. J. Cowley, A. J. Lough, J. M. Rawson and D. W. Stephan, *J. Am. Chem. Soc.*, 2013, **135**, 6446–6449; (j) M. K. Sharma, S. Blomeyer, B. Neumann, G. Stammler, A. Hinz, M. van Gastel, T. Glodde and R. S. Ghadwal, *Chem. Sci.*, 2020, **11**, 1975–

1984; (k) H. Cui, D. Xiao, L. Zhang, H. Ruan, Y. Fang, Y. Zhao, G. Tan, L. Zhao, G. Frenking, M. Driess and X. Wang, *Chem. Commun.*, 2020, **56**, 2167–2170; (l) K. Schwedtmann, S. Schulz, F. Hennersdorf, T. Strassner, E. Dmitrieva and J. J. Weigand, *Angew. Chem., Int. Ed.*, 2015, **54**, 11054–11058; (m) Z. Li, X. Chen, D. M. Andrada, G. Frenking, Z. Benkő, Y. Li, J. R. Harmer, C. Y. Su and H. Grützmacher, *Angew. Chem., Int. Ed.*, 2017, **56**, 5744–5749; (n) D. Rottschäfer, B. Neumann, H. G. Stammler and R. S. Ghadwal, *Chem.–Eur. J.*, 2017, **23**, 9044–9047.

6 (a) L. Weber, F. Ebeler and R. S. Ghadwal, *Coord. Chem. Rev.*, 2022, **461**, 214499; (b) R. S. Ghadwal, *Acc. Chem. Res.*, 2022, **55**, 457; (c) L. Weber, *Chem. Rev.*, 1992, **92**, 1839–1906; (d) N. Djawed and O. Andreas, *Eur. J. Inorg. Chem.*, 2016, 709–717; (e) R. C. Fischer and P. P. Power, *Chem. Rev.*, 2010, **110**, 3877–3923; (f) H.-L. Peng, J. L. Payton, J. D. Protasiewicz and M. C. Simpson, *J. Phys. Chem. A*, 2009, **113**, 7054–7063; (g) T. Sasamori and N. Tokitoh, *Dalton Trans.*, 2008, 1395–1408; (h) T. Busch, W. W. Schoeller, E. Niecke, M. Nieger and H. Westermann, *Inorg. Chem.*, 1989, **28**, 4334–4340; (i) L. P. Ho, A. Nasr, P. G. Jones, A. Altun, F. Neese, G. Bistoni and M. Tamm, *Chem.–Eur. J.*, 2018, **24**, 18922–18932.

7 M. Yoshifuji, I. Shima, N. Inamoto, K. Hirotsu and T. Higuchi, *J. Am. Chem. Soc.*, 1981, **103**, 4587–4589.

8 (a) A. H. Cowley, J. E. Kilduff, T. H. Newman and M. Pakulski, *J. Am. Chem. Soc.*, 1982, **104**, 5820–5821; (b) M. Yoshifuji, *Eur. J. Inorg. Chem.*, 2016, 607–615; (c) L. L. Liu, L. L. Cao, J. Zhou and D. W. Stephan, *Angew. Chem., Int. Ed.*, 2019, **58**, 273–277; (d) N. Hayakawa, K. Sadamori, S. Tsujimoto, M. Hatanaka, T. Wakabayashi and T. Matsuo, *Angew. Chem., Int. Ed.*, 2017, **56**, 5765–5769; (e) R. C. Smith, E. Urnezius, K.-C. Lam, A. L. Rheingold and J. D. Protasiewicz, *Inorg. Chem.*, 2002, **41**, 5296–5299; (f) L. P. Ho, A. Nasr, P. G. Jones, A. Altun, F. Neese, G. Bistoni and M. Tamm, *Chem.–Eur. J.*, 2018, **24**, 18922–18932; (g) E. Niecke, R. Rüger, M. Lysek, S. Pohl and W. Schoeller, *Angew. Chem., Int. Ed. Engl.*, 1983, **22**, 486–487; (h) S.-S. Asami, M. Okamoto, K. Suzuki and M. Yamashita, *Angew. Chem., Int. Ed.*, 2016, **55**, 12827–12831.

9 (a) M. Culcasi, G. Gronchi, J. Escudie, C. Couret, L. Pujol and P. Tordo, *J. Am. Chem. Soc.*, 1986, **108**, 3130–3132; (b) T. Sasamori, E. Mieda, N. Nagahora, K. Sato, D. Shiomi, T. Takui, Y. Hosoi, Y. Furukawa, N. Takagi, S. Nagase and N. Tokitoh, *J. Am. Chem. Soc.*, 2006, **128**, 12582–12588; (c) S.-s. Asami, S. Ishida, T. Iwamoto, K. Suzuki and M. Yamashita, *Angew. Chem., Int. Ed.*, 2017, **56**, 1658–1662; (d) A. J. Bard, A. H. Cowley, J. E. Kilduff, J. K. Leland, N. C. Norman, M. Pakulski and G. A. Heath, *J. Chem. Soc., Dalton Trans.*, 1987, 249–251; (e) S. Shah, S. C. Burdette, S. Swavey, F. L. Urbach and J. D. Protasiewicz, *Organometallics*, 1997, **16**, 3395–3400; (f) N. Nagahora, T. Sasamori, Y. Hosoi, Y. Furukawa and N. Tokitoh, *J. Organomet. Chem.*, 2008, **693**, 625–632.

10 (a) M. K. Sharma, D. Rottschäfer, S. Blomeyer, B. Neumann, H.-G. Stammler, M. van Gastel, A. Hinz and R. S. Ghadwal, *Chem. Commun.*, 2019, **55**, 10408–10411; (b) D. Rottschäfer,

M. K. Sharma, B. Neumann, H. G. Stammler, D. M. Andrada and R. S. Ghadwal, *Chem.–Eur. J.*, 2019, **25**, 8127–8134.

11 (a) W. Wang, C. Q. Xu, Y. Fang, Y. Zhao, J. Li and X. Wang, *Angew. Chem., Int. Ed.*, 2018, **57**, 9419–9424; (b) W. Wang, X. Wang, Z. Zhang, N. Yuan and X. Wang, *Chem. Commun.*, 2015, **51**, 8410–8413.

12 M. K. Sharma, D. Rottschäfer, B. Neumann, H. G. Stammler, S. Danes, D. M. Andrada, M. van Gastel, A. Hinz and R. S. Ghadwal, *Chem.–Eur. J.*, 2021, **27**, 5803–5809.

13 (a) L. Tuscher, C. Ganesamoorthy, D. Bläser, C. Wölper and S. Schulz, *Angew. Chem., Int. Ed.*, 2015, **54**, 10657–10661; (b) L. Tuscher, C. Helling, C. Ganesamoorthy, J. Krüger, C. Wölper, W. Frank, A. S. Nizovtsev and S. Schulz, *Chem.–Eur. J.*, 2017, **23**, 12297–12304; (c) L. Tuscher, C. Helling, C. Wölper, W. Frank, A. S. Nizovtsev and S. Schulz, *Chem.–Eur. J.*, 2018, **24**, 3241–3250.

14 J. M. Goicoechea and H. Grützmacher, *Angew. Chem., Int. Ed.*, 2018, **57**, 16968–16994.

15 (a) M. K. Sharma, C. Wölper, G. Haberhauer and S. Schulz, *Angew. Chem., Int. Ed.*, 2021, **60**, 6784–6790; (b) M. K. Sharma, C. Wölper, G. Haberhauer and S. Schulz, *Angew. Chem., Int. Ed.*, 2021, **60**, 21784–21788; (c) M. K. Sharma, C. Wölper and S. Schulz, *Dalton Trans.*, 2022, **51**, 1612–1616; (d) M. K. Sharma, P. Dhawan, C. Helling, C. Wölper and S. Schulz, *Chem.–Eur. J.*, 2022, e202200444.

16 (a) L. Liu, D. A. Ruiz, F. Dahcheh, G. Bertrand, R. Suter, A. M. Tondreauc and H. Grützmacher, *Chem. Sci.*, 2016, **7**, 2335–2341; (b) D. Wilson, W. Myers and J. M. Goicoechea, *Dalton Trans.*, 2020, **49**, 15249–15255.

17 Full crystallographic data of all structurally characterized compounds described herein as well as central bond lengths and angles (Tables S1–S3 and Fig. S37–S44) are given in the Supporting Information.†

18 (a) P. Pyykkö and M. Atsumi, *Chem.–Eur. J.*, 2009, **15**, 12770–12779; (b) P. Pyykkö and M. Atsumi, *Chem.–Eur. J.*, 2009, **15**, 186–197.

19 M. Stender, B. E. Eichler, N. J. Hardman, P. P. Power, J. Prust, M. Noltemeyer and H. W. Roesky, *Inorg. Chem.*, 2001, **40**, 2794–2799.

20 The ORCA quantum chemistry package was used and details regarding the quantum chemical calculations are given in the ESI.†(a) F. Neese, *Wiley Interdiscip. Rev.: Comput. Mol. Sci.*, 2018, **8**, 1–6; (b) F. Neese, *Wiley Interdiscip. Rev.: Comput. Mol. Sci.*, 2012, **2**, 73–78

21 H. Weinert, C. Wölper and S. Schulz, *Organometallics*, 2021, **40**, 3486–3495.

22 (a) N. Hayakawa, K. Sadamori, S. Tsujimoto, M. Hatanaka, T. Wakabayashi and T. Matsuo, *Angew. Chem., Int. Ed.*, 2017, **56**, 5765–5769; (b) D. Dhara, P. Kalita, S. Mondal, R. S. Narayanan, K. R. Mote, V. Huch, M. Zimmer, C. B. Yildiz, D. Scheschkewitz, V. Chandrasekhar and A. Jana, *Chem. Sci.*, 2018, **9**, 4235–4243.

23 C. Helling, C. Wölper and S. Schulz, *Eur. J. Inorg. Chem.*, 2020, 4225–4235.

24 (a) C. Helling, C. Wölper and S. Schulz, *J. Am. Chem. Soc.*, 2018, **140**, 5053–5056; (b) J. Krüger, C. Ganesamoorthy, L. John, C. Wölper and S. Schulz, *Chem.–Eur. J.*, 2018, **24**, 9157–9164; (c) J. Schoening, L. John, C. Wölper and S. Schulz, *Dalton Trans.*, 2019, **48**, 17729–17734.

25 (a) J. Krüger, C. Wölper, L. John, L. Song, P. R. Schreiner and S. Schulz, *Eur. J. Inorg. Chem.*, 2019, 1669–1678; (b) L. Tuscher, C. Helling, C. Ganesamoorthy, J. Krüger, C. Wölper, W. Frank, A. S. Nizovtsev and S. Schulz, *Chem.–Eur. J.*, 2017, **23**, 12297–12304; (c) C. Ganesamoorthy, J. Krüger, C. Wölper, A. S. Nizovtsev and S. Schulz, *Chem.–Eur. J.*, 2017, **23**, 2461–2468; (d) L. Tuscher, C. Ganesamoorthy, D. Bläser, C. Wölper and S. Schulz, *Angew. Chem., Int. Ed.*, 2015, **54**, 10657–10661.

26 A. E. Reed, L. A. Curtiss and F. Weinhold, *Chem. Rev.*, 1988, **88**, 899–926.

27 (a) S. Burck, K. Götz, M. Kaupp, M. Nieger, J. Weber, J. S. a. d. Günne and D. Gudat, *J. Am. Chem. Soc.*, 2009, **131**, 10763–10774; (b) V. Gandon, J. B. Bourg, F. S. Tham, W. W. Schoeller and G. Bertrand, *Angew. Chem., Int. Ed.*, 2008, **47**, 155–159.